Epigenetic Control of rDNA Loci in Response to Intracellular Energy Status

Akiko Murayama,[1,2,5,6] Kazuji Ohmori,[1,6] Akiko Fujimura,[1] Hiroshi Minami,[4] Kayoko Yasuzawa-Tanaka,[1] Takao Kuroda,[1] Shohei Oie,[1] Hiroaki Daitoku,[2] Mitsuru Okuwaki,[3] Kyosuke Nagata,[3] Akiyoshi Fukamizu,[2] Keiji Kimura,[1] Toshiyuki Shimizu,[4] and Junn Yanagisawa[1,*]
[1]Graduate School of Life and Environmental Sciences
[2]Center for Tsukuba Advanced Research Alliance
[3]Graduate School of Comprehensive Human Sciences and Institute of Basic Medical Sciences
University of Tsukuba, 1-1-1 Tennodai, Tsukuba 305-8572, Japan
[4]International Graduate School of Arts and Sciences, Yokohama City University, Yokohama, Kanagawa 230-0045, Japan
[5]PRESTO, JST, 4-1-8 Honcho Kawaguchi, Saitama, Japan
[6]These authors contributed equally to this work.
*Correspondence: junny@agbi.tsukuba.ac.jp
DOI 10.1016/j.cell.2008.03.030

SUMMARY

Intracellular energy balance is important for cell survival. In eukaryotic cells, the most energy-consuming process is ribosome biosynthesis, which adapts to changes in intracellular energy status. However, the mechanism that links energy status and ribosome biosynthesis is largely unknown. Here, we describe eNoSC, a protein complex that senses energy status and controls rRNA transcription. eNoSC contains Nucleomethylin, which binds histone H3 dimethylated Lys9 in the rDNA locus, in a complex with SIRT1 and SUV39H1. Both SIRT1 and SUV39H1 are required for energy-dependent transcriptional repression, suggesting that a change in the NAD^+/NADH ratio induced by reduction of energy status could activate SIRT1, leading to deacetylation of histone H3 and dimethylation at Lys9 by SUV39H1, thus establishing silent chromatin in the rDNA locus. Furthermore, eNoSC promotes restoration of energy balance by limiting rRNA transcription, thus protecting cells from energy deprivation-dependent apoptosis. These findings provide key insight into the mechanisms of energy homeostasis in cells.

INTRODUCTION

Ribosome production is a major biosynthetic and energy-consuming activity of eukaryotic cells. Ribosome biosynthesis adapts rapidly to changes in intracellular energy status. Conditions of energy starvation or glucose deprivation—when cellular AMP/ATP ratio is increased—lead to the activation of the LKB1-AMPK (AMP-activated protein kinase) pathway (Hardie, 2004); this signaling inhibits mammalian TOR (target of rapamycin)/p70 S6 kinase activity, which is required for rapid and sustained serum-induced ribosome biosynthesis (Bhaskar and Hay, 2007). Inhibition of mTOR activity by AMPK suppresses energy expenditure and protects cells from energy deprivation-induced apoptosis (Inoki et al., 2003; Shaw et al., 2004). Anaerobic conditions also reduce cellular energy supply. Cells regulate energy demand by sensing the environmental concentration of hydrogen ions. H^+ produced under hypoxia promotes interactions between VHL and rDNA to reduce rRNA synthesis (Mekhail et al., 2006).

rRNA synthesis is tightly regulated in response to metabolic and environmental changes (Grummt, 2003; Moss et al., 2007). rRNA genes are present in multiple copies; therefore, rRNA synthesis could be modulated by varying transcription rate per gene or by varying the number of active genes. Exponentially growing cells use no more than half of their total complement of rRNA genes, and it has been shown in both mammalian cells and budding yeast that the number of active genes decreases when cells undergo transition from log to stationary phase (Claypool et al., 2004; Preuss and Pikaard, 2007; Sandmeier et al., 2002). In yeast, this gene inactivation is dependent on the histone deacetylase Rpd3 (Oakes et al., 2006). In mammalian cells, the chromatin-remodeling complex NoRC recruits HDAC1 and DNA methyltransferases to inactive rRNA gene repeats (Santoro et al., 2002). Furthermore, the activity level of rRNA genes is correlated with the type and extent of their chromatin modifications. Taken together, these data argue that epigenetic mechanisms control the ratio of active to inactive genes.

In yeast, heterochromatin formation at the ribosomal DNA (rDNA) locus is also controlled by Sir2p, an NAD^+-dependent deacetylase that removes acetyl groups from the N-terminal tails of histone H3 and H4 to regulate nucleosome and chromatin structure (Buck et al., 2002). Increasing the expression of Sir2p can extend the life span of yeast by suppressing homologous recombination between rDNA repeat sequences (Guarente, 2000). In human, the Sir2p homolog SIRT1 deacetylates transcription factors such as FOXOs, p53, and NF-κB (Yang et al., 2006). SIRT1 is inducibly transcribed in response to calorie restriction
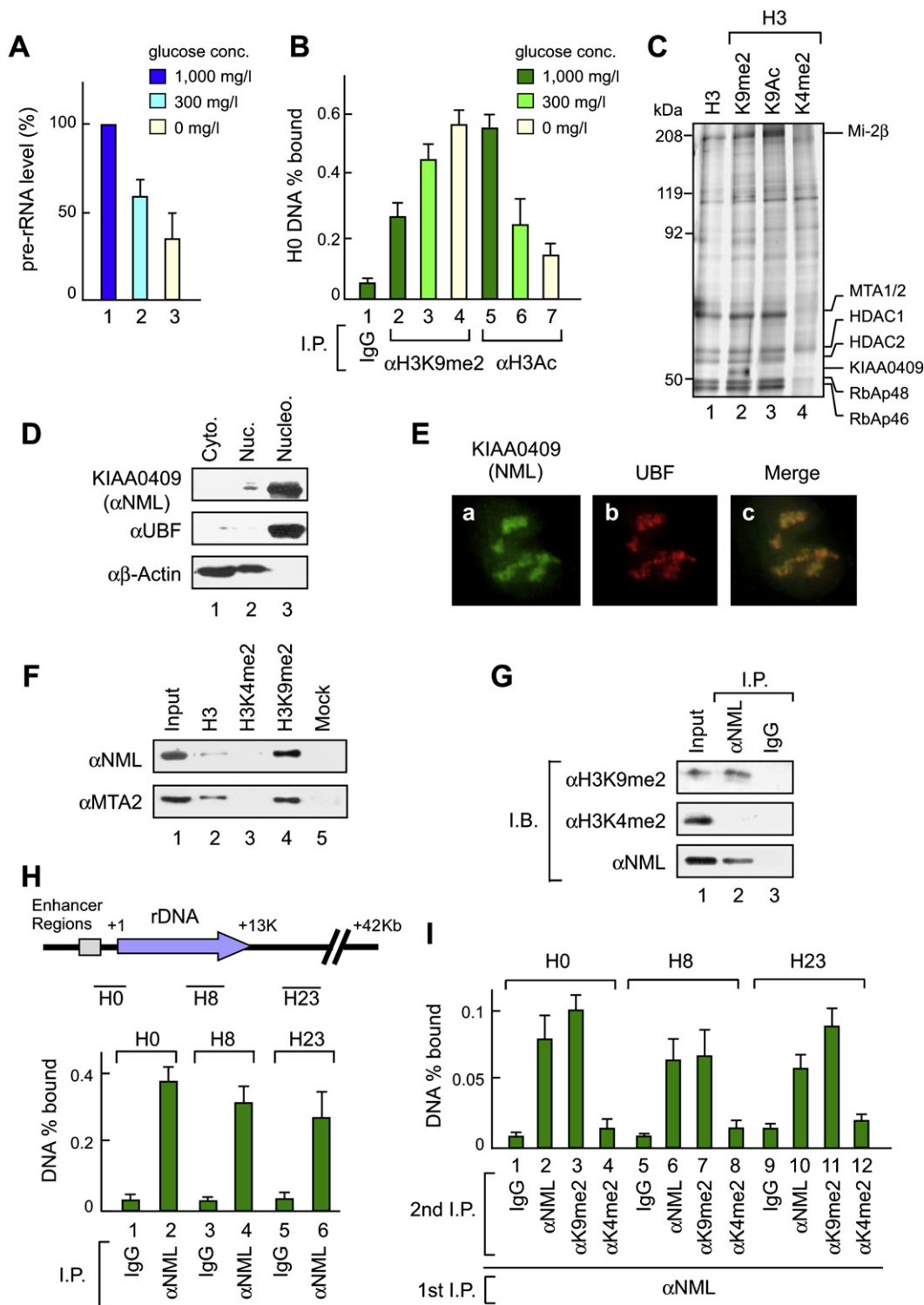
Figure 1. NML Binds to Histone H3 Dimethylated at Lys9 at the rDNA Locus

(A) Downregulation of pre-rRNA levels by glucose deprivation. HeLa cells were cultured in medium containing 1000, 300, or 0 mg/l glucose, and pre-rRNA levels were determined after 24 hr by RT-qPCR, using primers that are specific for the 5′ external transcribed spacer (ETS) of pre-rRNA and normalizing for cell count. Values are means ± SD for triplicates.

(B) Glucose deprivation induces heterochromatin formation at the rDNA locus. HeLa cells were cultured in medium containing 1000, 300, or 0 mg/l glucose for 24 hr. ChIP analysis was performed to examine histone modifications at rRNA promoters. Immunoprecipitated DNA was analyzed by qPCR using H0 primers (see Figure 1H) and normalized to input DNA. Values are means ± SD for triplicates.

(CR) or fasting (Cohen et al., 2004; Nemoto et al., 2004), suggesting a broad role in mammalian physiology as a mediator of adaptation to nutrient deprivation.

Here, we identify a protein complex, eNoSC (energy-dependent *n*ucleolar *s*ilencing *c*omplex), that contains a previously uncharacterized protein, termed Nucleomethylin (NML), as well as SIRT1 and SUV39H1. Our results suggest that an energy-dependent change in the NAD$^+$/NADH ratio regulates eNoSC, allowing the complex to couple changing energy status with level of rRNA synthesis. In addition, by limiting ribosome biogenesis, eNoSC promotes the restoration of energy balance and protects cells from energy deprivation-dependent apoptosis.

RESULTS

A Nucleolar Protein, NML, Binds to H3K9me2 at the rDNA Locus

Glucose deprivation activates LKB1-AMPK signaling and leads to the inhibition of ribosome biogenesis (Shaw et al., 2004). Glucose deprivation also reduces rRNA synthesis in HeLa cells (Figure 1A). Because HeLa cells do not express LKB1 (Tiainen et al., 1999), this result raises the possibility that, in addition to the LKB1-AMPK pathway, there are other pathways that control cellular energy balance.

The LKB1-AMPK pathway reduces the transcription rate of rRNA genes. In contrast, recent reports mention the importance of epigenetic regulation of rDNA (McStay, 2006). Thus, we next investigated whether glucose removal affects the chromatin structure on rDNA locus. We analyzed the levels of methylation at Lys9 and acetylation of histone H3 at the rDNA locus by using quantitative chromatin immunoprecipitation (ChIP) with primers that amplify the rRNA genes (H0; Figure 1H). Glucose reduction induced the deacetylation and dimethylation at Lys9 of histone H3 in rRNA genes (Figure 1B).

To elucidate the mechanisms which link cellular energy status and epigenetic status of rDNA, we purified proteins that bind to histone H3 dimethylated at Lys9 (H3K9me2) from HeLa nuclear extracts, using differentially modified N-terminal tails of histone H3 peptides. Using mass spectrometry, we identified a protein that specifically binds to the H3K9me2 peptide as KIAA0409 (accession number BC001071, GeneID 23378) (Figure 1C). According to a recent proteomic analysis of nucleolar proteins, KIAA0409 localizes in the nucleolus (Andersen et al., 2005). Subcellular fractionation using the Muramatsu method (Andersen et al., 2005; Muramatsu and Busch, 1964) and immunofluorescence studies confirmed that KIAA0409 is present in the nucleoli along with UBF (Figures 1D and 1E). Therefore, we designated KIAA0409 as NML.

Western blot analysis with anti-NML antibody (Figure S1 available online) and pull-down experiments revealed that this protein preferentially bound to the H3K9me2 peptide (Figures 1F and S2). NML specifically coimmunoprecipitates with Lys9-dimethylated but not with Lys4-dimethylated histone H3 (Figure 1G). ChIP and re-ChIP analysis using primers that amplify the rRNA gene promoter (H0), the 28S rRNA coding region (H8), or the noncoding region (H23) indicated that NML bound throughout the rDNA locus with H3K9me2 (Figures 1H and 1I). These observations suggest that NML binds to H3K9me2 in the silent rDNA clusters in vivo in the context of native chromatin.

NML Functions to Suppress rRNA Gene Transcription

Given that NML preferentially binds to silent rDNA clusters, it is possible that NML might have a suppressive function on rRNA transcription. Thus, we next examined pre-rRNA synthesis in various cell lines infected with adenovirus vector containing either NML (ad-NML) or LacZ (ad-LacZ) as a control. Infection of ad-NML resulted in a decrease of pre-rRNA levels in all cell lines tested (Figure 2A). Conversely, the level of pre-rRNA synthesis was increased in cells transfected with small-interfering RNAs against NML (NML siRNAs) (Figures 2B and 2C). We also performed nuclear run-on assays and confirmed that NML reduced the level of transcription (Figure 2D).

Next, we generated clones that stably expressed a small hairpin RNA against NML (NML shRNA), control LacZ (control), or FLAG-NML (NML stable) (Figure 2E). The growth rates of these cell lines were almost the same (data not shown). RT quantitative PCR (qPCR) analysis confirmed the enhancement of pre-rRNA synthesis in NML shRNA clones and reduction in the NML stable clones (Figure 2F). In addition, NML reduces the level of protein synthesis in an NML-dose-dependent manner (Figure 2G). Taken together, these observations suggest that NML associates with H3K9me2 in heterochromatic clusters in rDNA and suppresses rRNA synthesis and ribosome biogenesis. ChIP analysis revealed that increasing levels of NML caused a dose-dependent reduction of the acetylation and elevation of the Lys9 methylation of histone H3 (Figure 2H). These results indicate that alteration of NML levels changes the ratio between active and silent states in the rDNA repeats.

(C) Protein purification was performed from HeLa S3 cell nuclear extracts using histone H3 peptides with different modifications (K9me2, K9Ac, or K4me2). Bound proteins were resolved by SDS-PAGE, visualized by silver staining, and analyzed by mass spectrometry.

(D) NML is enriched in the nucleolar fraction. HeLa cells were fractionated into cytosolic (Cyto.), nuclear (Nuc.), and nucleolar fraction (Nucleo.) and endogenous proteins of each fraction were analyzed by immunoblotting using anti-NML, anti-UBF, and anti-β-actin antibodies. UBF was used as a nucleolar marker.

(E) NML localizes in the nucleolus. Endogenous NML and UBF were visualized by immunofluorescence in HeLa cells using anti-NML and anti-UBF antibodies.

(F) Endogenous NML associates with H3K9me2 peptide. Nuclear extracts from HeLa S3 cells were used in the peptide pull-down assays and analyzed by immunoblotting with anti-NML and anti-MTA2 antibodies.

(G) Endogenous NML associates with H3K9me2 nucleosomes. Mononucleosomal fraction was purified from HeLa cells and subjected to immunoprecipitation with anti-NML antibody. The immunoprecipitates were analyzed by immunoblotting with anti-H3K9me2, anti-H3K4me2, and anti-NML antibodies.

(H) Upper panel: The structure of the human rDNA repeat. The locations of primer pairs (H0, H8, and H23) are shown below the diagram of the human rDNA repeat. Lower panel: Endogenous NML binds across the entire rDNA in vivo. ChIP assay using HeLa cells was performed with normal IgG and anti-NML antibody. Values are means ± SD for triplicates.

(I) Endogenous NML colocalizes with H3K9me2 on rDNA. Re-ChIP experiments using HeLa cells were performed by a first immunoprecipitation with anti-NML antibody, followed by a second precipitation with anti-NML, anti-H3K9me2, and anti-H3K4me2 antibodies. Values are means ± SD for triplicates.
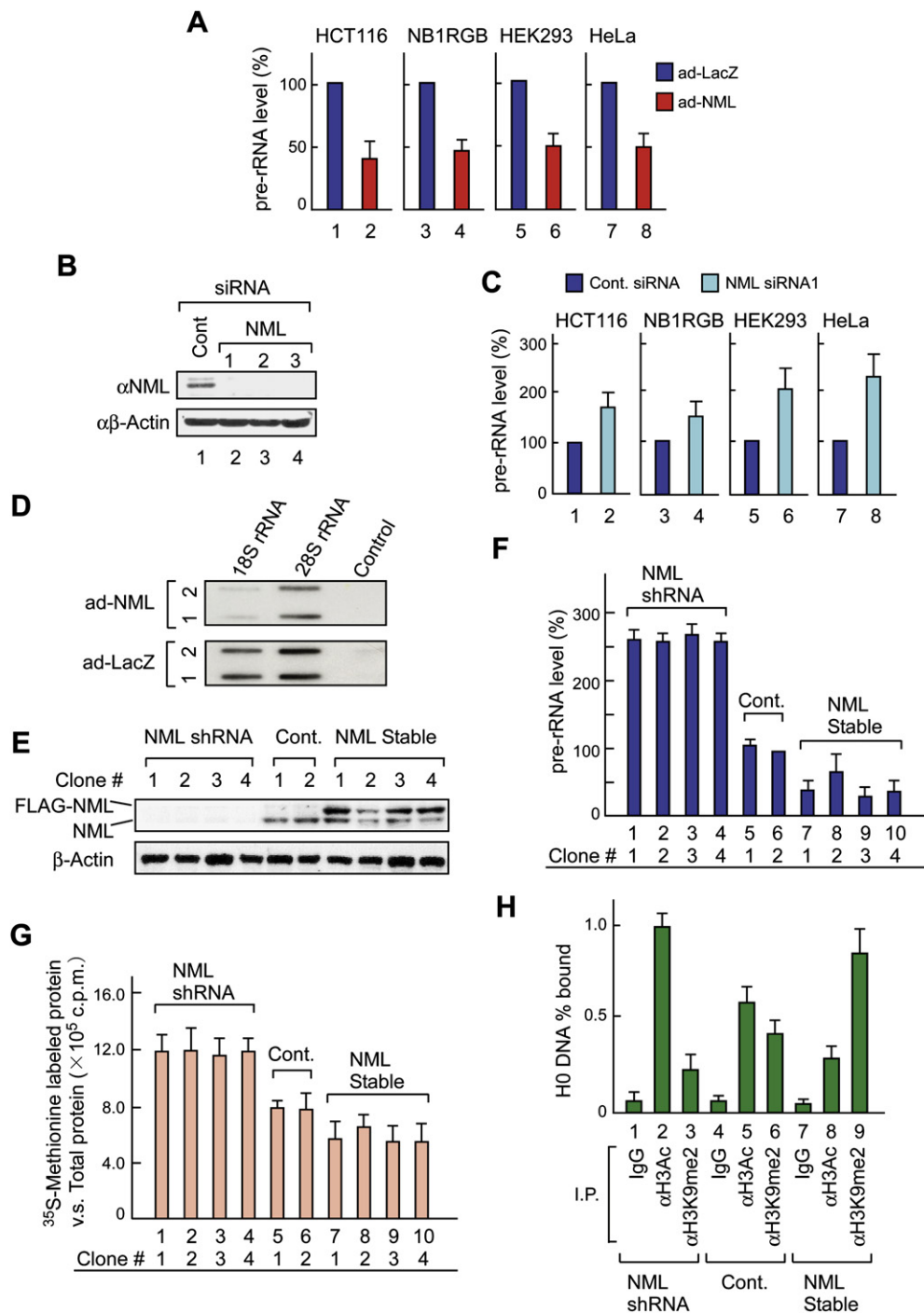
Figure 2. NML Represses Pre-rRNA Synthesis

(A) NML expression reduces pre-rRNA level in various types of cells. HCT116, NB1RGB, HEK293, and HeLa cells were transiently infected with ad-NML or ad-LacZ adenoviruses. After 24 hr, pre-rRNA level was determined by RT-qPCR. Values are means ± SD for triplicates.

(B) siRNAs efficiently knock down endogenous NML. HEK293 cells were transfected with siRNAs against NML. The level of endogenous NML protein was detected by immunoblotting.

(C) Knockdown of NML increases pre-rRNA level. HCT116, NB1RGB, HEK293, and HeLa cells were transfected with siRNA against NML. Forty-eight hours after transfection, total RNA was isolated, and pre-rRNA level was analyzed by RT-qPCR. Values are means ± SD for triplicates.

(D) NML expression represses rRNA transcription. Nuclear run-on assays were performed to measure transcription of 47S rRNA in ad-LacZ or ad-NML infected HeLa cells. The assays were performed in duplicate.

NML Associates with SIRT1

To investigate the molecular bases for the functions of NML, control or NML-overexpressing cells were treated with the histone deacetylase inhibitors, trichostatin A (TSA) and nicotinamide (NIA). TSA inhibits class I/II HDACs; NIA is known as a class III HDAC inhibitor and a potent inhibitor of SIRT1. As shown in Figure 3A, reduction of pre-rRNA levels by NML overexpression was prevented by NIA, but not by TSA, implicating SIRT1 in the NML-mediated inhibition of rRNA synthesis. Knockdown of endogenous SIRT1 by siRNAs increased pre-rRNA levels and prevented the NML-dependent repression (Figures 3B and 3C). Conversely, expression of SIRT1 decreased pre-rRNA levels and strengthened the NML-dependent repression (Figure 3C).

We next tested the interaction between NML and SIRT1 by coimmunoprecipitation and found that SIRT1 interacts with NML (Figure 3D). ChIP analysis using H0, H8, or H23 primers showed that SIRT1 associated with chromatin throughout the rDNA locus (Figure S3). In addition, re-ChIP analysis revealed that a protein complex containing NML and SIRT1 associates with the silent chromatin region of rDNA (Figure 3E). The binding of SIRT1 to rDNA was abrogated by NML siRNA treatment (Figures 3F and S4). Interestingly, SIRT1 siRNA also reduced the binding of NML to the rDNA locus (Figure 3F). These results indicate the coordinate binding of NML and SIRT1 to rDNA.

Expression of a deacetylase activity-deficient SIRT1 mutant, SIRT1(H355A), resulted in increased pre-rRNA levels and prevented the NML-dependent reduction of pre-rRNA levels (Figures 3G and S5), indicating that the deacetylase activity of SIRT1 is necessary for the repression of rRNA synthesis mediated by NML. SIRT1 preferentially deacetylates core histones H3 Lys9, H3 Lys14, and H4 Lys16 in vitro (Vaquero et al., 2004). A ChIP assay showed that reduction of SIRT1 protein level by siRNA increased the acetylation of histone H3 at the rDNA locus (Figure 3H). Interestingly, we also observed a decrease in Lys9 methylation of H3 as a result of SIRT1 knockdown (Figure 3H). This result implies that deacetylation at Lys9 of H3 is prerequisite for its methylation (Shankaranarayana et al., 2003). Considering these results together with the observation that NML knockdown also reduced the Lys9 methylation of H3 (Figure 2H), it appears that histone methyltransferases participate in the NML/SIRT1-mediated rRNA gene silencing.

NML Forms a Ternary Complex with SIRT1 and SUV39H1

It is known that Lys9 of histone H3 is methylated by histone methyltransferases such as SUV39H1, EZH2, and G9a (Lachner and Jenuwein, 2002). G9a is involved in the activation of rRNA gene transcription (Yuan et al., 2007). Therefore, we investigated the possibility of an interaction between NML and either

SUV39H1 or EZH2 and found that NML preferentially associates with SUV39H1 (Figure 4A). SUV39H1 siRNA prevented the NML-dependent repression of rRNA synthesis (Figures 4B and 4C). On the other hand, expression of SUV39H1 decreased pre-rRNA levels (Figure 4D). The SUV39H1-dependent reduction of pre-rRNA levels requires the methyltransferase activity of SUV39H1; overexpression of SUV39H1(R235H), a methyltransferase activity-deficient mutant, resulted in increased pre-rRNA levels (Figures 4D and S6). A ChIP assay showed that reduction of SUV39H1 protein levels decreased the Lys9 methylation and increased the acetylation of histone H3 at the rDNA locus (Figure 4E). Because knockdown of SUV39H1 increased the acetylation of H3, it is possible that SUV39H1 is involved in the recruitment of NML and SIRT1. Consistent with this idea, the binding of NML and SIRT1 to rDNA was abrogated by SUV39H1 siRNA (Figure 4F). These results indicate the coordinate binding of NML, SIRT1, and SUV39H1 to rDNA.

To investigate the possibility that these proteins form a single protein complex, the protein complex containing both NML and SUV39H1 was sequentially immunoprecipitated by antibodies. Immunoblotting of the precipitate with anti-SIRT1 antibody demonstrated the presence of SIRT1 (Figure 4G), indicating that NML formed a ternary complex with both SIRT1 and SUV39H1. To confirm this interaction among the endogenous proteins, we immunoprecipitated the protein complex from HeLa cell extracts using anti-NML antibody and identified SIRT1 and SUV39H1 in the precipitates (Figure 4H). In purification experiments using H3K9me2 peptide, NML, SIRT1, and SUV39H1 were copurified (Figure 4I). Our observations indicate that an NML/SIRT1/SUV39H1 protein complex suppresses rRNA gene transcription by establishing silent chromatin at the rDNA locus.

NML Protects Cells from Cell Death Induced by Glucose Deprivation

In mammalian cells, CR decreases cellular ATP concentration and increases the $NAD^+/NADH$ ratio (Guarente and Picard, 2005). According to our observations and the fact that the $NAD^+/NADH$ ratio regulates the deacetylase activity of SIRT1, it is possible that the NML/SIRT1/SUV39H1 complex participates in CR-induced repression of rRNA gene transcription. ChIP analysis revealed that the binding of NML and SIRT1 to the rDNA locus increased during glucose deprivation (Figure 5A). In addition, neither downregulation of pre-rRNA levels nor alteration of histone modifications induced by glucose deprivation were observed in cells treated with siRNA against NML, SIRT1, or SUV39H1 (Figures 5B and 5C). Thus, the NML/SIRT1/SUV39H1 complex participates in the downregulation of rRNA transcription under CR. Consequently, we designated the NML/SIRT1/SUV39H1 complex as eNoSC.

(E) Protein level of NML in HeLa cells stably expressing FLAG-NML (NML stable), shRNA against NML (NML shRNA), or control cells (Cont.) was determined by immunoblotting using anti-NML antibody.
(F) NML decreases pre-rRNA level in a dose-dependent manner. Pre-rRNA level in control, NML stable, or NML shRNA HeLa cells was determined by RT-qPCR. Values are means ± SD for triplicates.
(G) Expression of NML decreases rate of protein synthesis. The indicated HeLa cells were incubated with ^{35}S-methionine for 4 hr; incorporation of ^{35}S-methionine into protein was measured by scintillation counting and normalized to total protein levels. Values are means ± SD for triplicates.
(H) Overexpression of NML induces deacetylation and dimethylation in histone H3 at Lys9. ChIP analysis was performed to determine histone modifications on the rRNA promoter (H0) using the indicated HeLa cells. Values are means ± SD for triplicates.
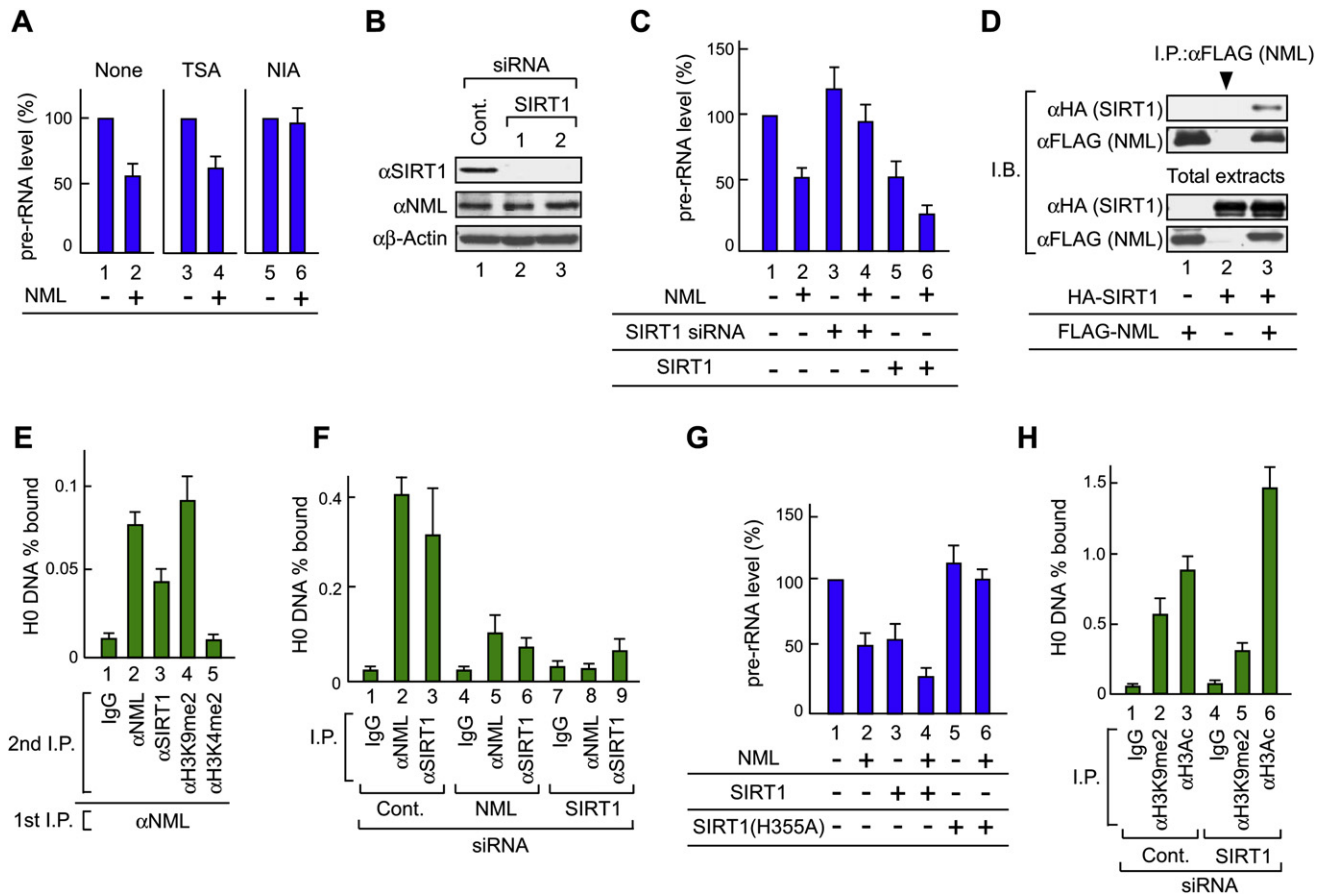
Figure 3. NAD$^+$-Dependent Histone Deacetylase SIRT1 Is Required for NML-Mediated Repression of rRNA Synthesis

(A) NIA inhibits NML-mediated rRNA repression. HEK293 cells transfected with NML or control plasmid were cultured for 6 hr in medium containing 40 nM TSA or 5 mM NIA, and pre-rRNA levels were measured by RT-qPCR. Values are means ± SD for triplicates.

(B) siRNAs efficiently knock down endogenous SIRT1. HEK293 cells were transfected with siRNAs against SIRT1. The levels of endogenous SIRT1 and NML proteins were examined by immunoblotting.

(C) SIRT1 knockdown restores repression of rRNA synthesis by NML. HEK293 cells were transfected in combination with NML, SIRT1 plasmids, and SIRT1 siRNA as indicated. Forty-eight hours after transfection, pre-rRNA levels were determined by RT-qPCR. Values are means ± SD for triplicates.

(D) NML interacts with SIRT1. HEK293 cells were transfected with the indicated plasmids. The cell lysates were immunoprecipitated by anti-FLAG antibody and immunoblotted with anti-HA or anti-FLAG antibody.

(E) Endogenous NML and SIRT1 associate together with the rDNA locus. Re-ChIP experiments were performed using HeLa cells by first immunoprecipitating with anti-NML antibody, followed by a second precipitation with the indicated antibodies. Values are means ± SD for triplicates.

(F) Coordinated binding of endogenous NML and SIRT1 to rDNA. Association of NML or SIRT1 to rDNA was analyzed by ChIP using anti-NML and anti-SIRT1 antibodies in HEK293 cells following treatment with either NML siRNA or SIRT1 siRNA. Values are means ± SD for triplicates.

(G) SIRT1 potentiates reduction of pre-rRNA level via its deacetylase activity. HEK293 cells were transiently transfected with NML, SIRT1, or catalytically inactive SIRT1(H355A) plasmid. Forty-eight hours after transfection, pre-rRNA levels were determined by RT-qPCR. Values are means ± SD for triplicates.

(H) SIRT1 is required for heterochromatin formation at the rDNA locus. Modification of histones at rRNA promoters was analyzed by ChIP in HEK293 cells following treatment with control or SIRT1 siRNA. Values are means ± SD for triplicates.

Next, we performed parallel timecourse studies of pre-rRNA levels and total cellular ATP levels in control and NML shRNA cells. As shown in Figure 5D, in the absence of glucose, pre-rRNA levels in NML shRNA cells reduced more slowly than those in the control cells. In contrast, the total cellular ATP levels in NML shRNA cells decreased faster than those in control cells. These observations suggest that eNoSC restores energy levels under low-glucose conditions.

TUNEL assay and poly(ADP-ribose) polymerase 1 (PARP-1) cleavage assay revealed that insufficient intracellular energy induced apoptosis (Figures 5E and 5F). Thus, we next measured the percentage of dead cells in populations of HEK293 cells transfected with either indicated siRNAs or NML expression vector after various intervals of glucose deprivation (Figure 5G). When glucose was withdrawn, cells treated with siRNA against NML, SIRT1, or SUV39H1 died rapidly as compared with control siRNA-treated cells (Figure 5G). Knockdown of the components of eNoSC reduced the tolerance of low-glucose conditions (Figure 5H). The same results were obtained when we used HeLa cells (Figure S7). Conversely,
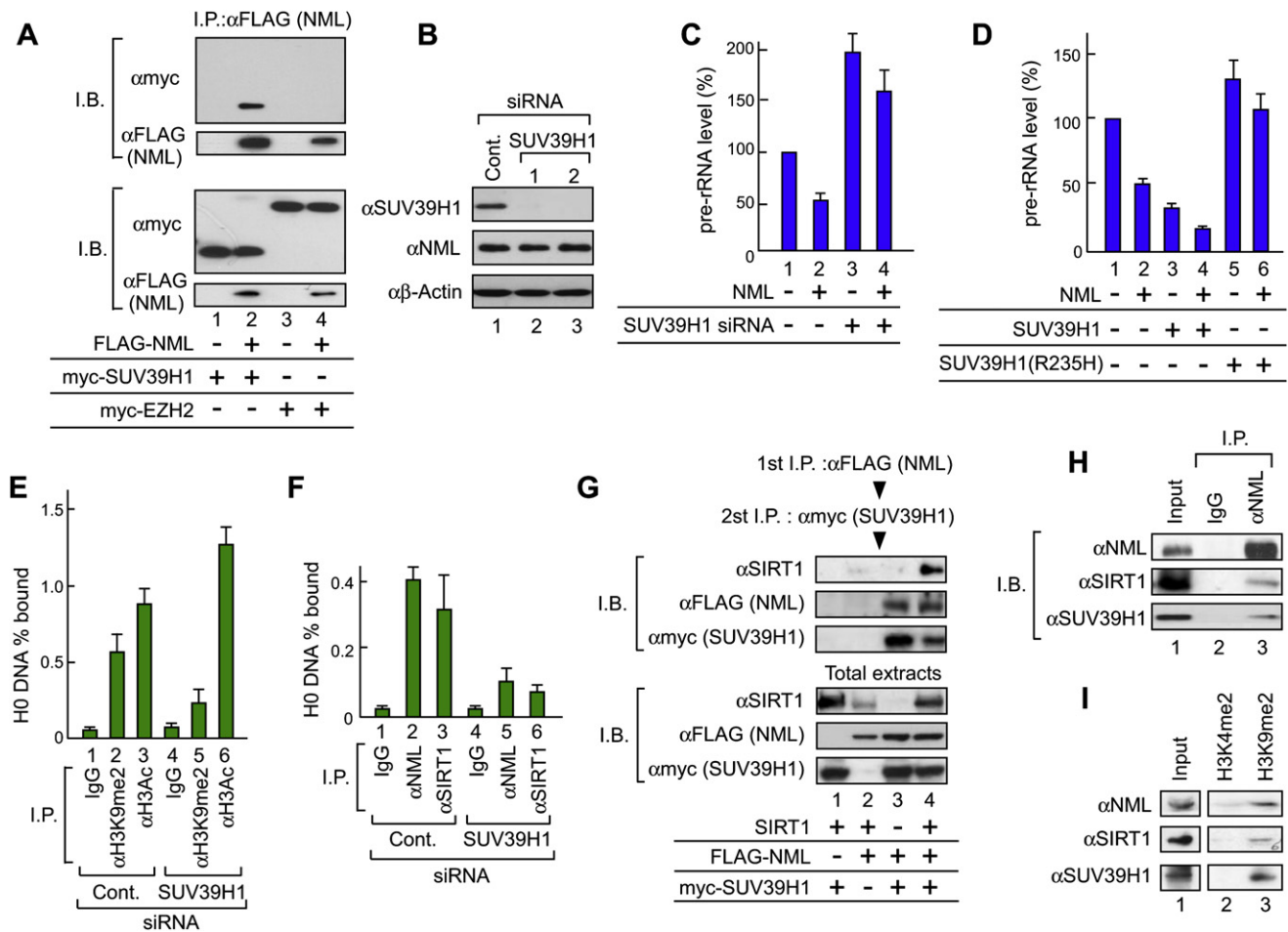
Figure 4. NML/SIRT1/SUV39H1 Complex Suppresses rRNA Synthesis

(A) NML interacts with SUV39H1. HEK293 cells were transfected with FLAG-NML, myc-SUV39H1, or myc-EZH2 as indicated. 24 hr after transfection, the cell lysates were immunoprecipitated with anti-FLAG antibody and immunoblotted with anti-FLAG or anti-myc antibody.

(B) The siRNAs efficiently knock down endogenous SUV39H1. HEK293 cells were transfected with siRNAs against SUV39H1. The level of endogenous SUV39H1 protein was examined by immunoblotting.

(C) SUV39H1 knockdown restores repression of pre-rRNA synthesis by NML. HEK293 cells were transfected in combination with NML plasmid and SUV39H1 siRNA as indicated. Forty-eight hours after transfection, pre-rRNA levels were determined by RT-qPCR. Values are means ± SD for triplicates.

(D) SUV39H1 represses pre-rRNA synthesis via its histone methyltransferase activity. HEK293 cells were transiently transfected with NML, SUV39H1, or SUV39H1(R235H) plasmid. Forty-eight hours after transfection, pre-rRNA levels were determined by RT-qPCR. Values are means ± SD for triplicates.

(E) SUV39H1 is required for heterochromatin formation at the rDNA locus. Modification of histone on rDNA was analyzed by ChIP using the indicated antibodies in HEK293 cells, following treatment with control or SUV39H1 siRNA. Immunoprecipitated DNA was analyzed by qPCR using H0 primers. Values are means ± SD for triplicates.

(F) SUV39H1 is required for binding of NML and SIRT1 to rDNA locus. Control or SUV39H1 siRNA-treated HEK293 cells were analyzed by ChIP assay using anti-NML or anti-SIRT1 antibody. Values are means ± SD for triplicates.

(G) NML forms a ternary complex with SIRT1 and SUV39H1. HEK293 cells were transfected in combination with FLAG-NML, myc-SUV39H1, and SIRT1 plasmids as indicated. FLAG-NML was immunoprecipitated using anti-FLAG antibody. NML/SIRT1/SUV39H1 complex was eluted using FLAG peptides then immunoprecipitated with anti-myc antibody. SIRT1 in immunoprecipitates was detected by immunoblotting.

(H) Endogenous NML associates with SIRT1 and SUV39H1. The cell lysates from HeLa cells were prepared and immunoprecipitated with normal rabbit IgG or anti-NML antibody and immunoblotted using antibodies against SIRT1 and SUV39H1.

(I) SIRT1 and SUV39H1 associate with H3K9me2 peptide. Whole-cell extracts of HeLa cells were pulled down with the indicated peptide. Pull-down assay was performed in a buffer containing 50 mM Tris-HCl (pH 7.2), 150 mM NaCl, 0.1% NP-40, 1 mM DTT, and 2 mM EDTA. Bound protein was resolved by 10% SDS-PAGE and analyzed by immunoblotting with anti-NML, anti-SUV39H1, and anti-SIRT1 antibodies.

NML expression protected cells from apoptosis (Figures 5G and 5H). These results indicate that eNoSC-mediated rDNA silencing protects cells from energy deprivation-induced apoptosis.

The Methyltransferase-like Domain of NML Plays an Important Role in Repression of rRNA Transcription

Sequence analysis demonstrates that the N-terminal domain of NML shows no obvious domain structure; however, it is required
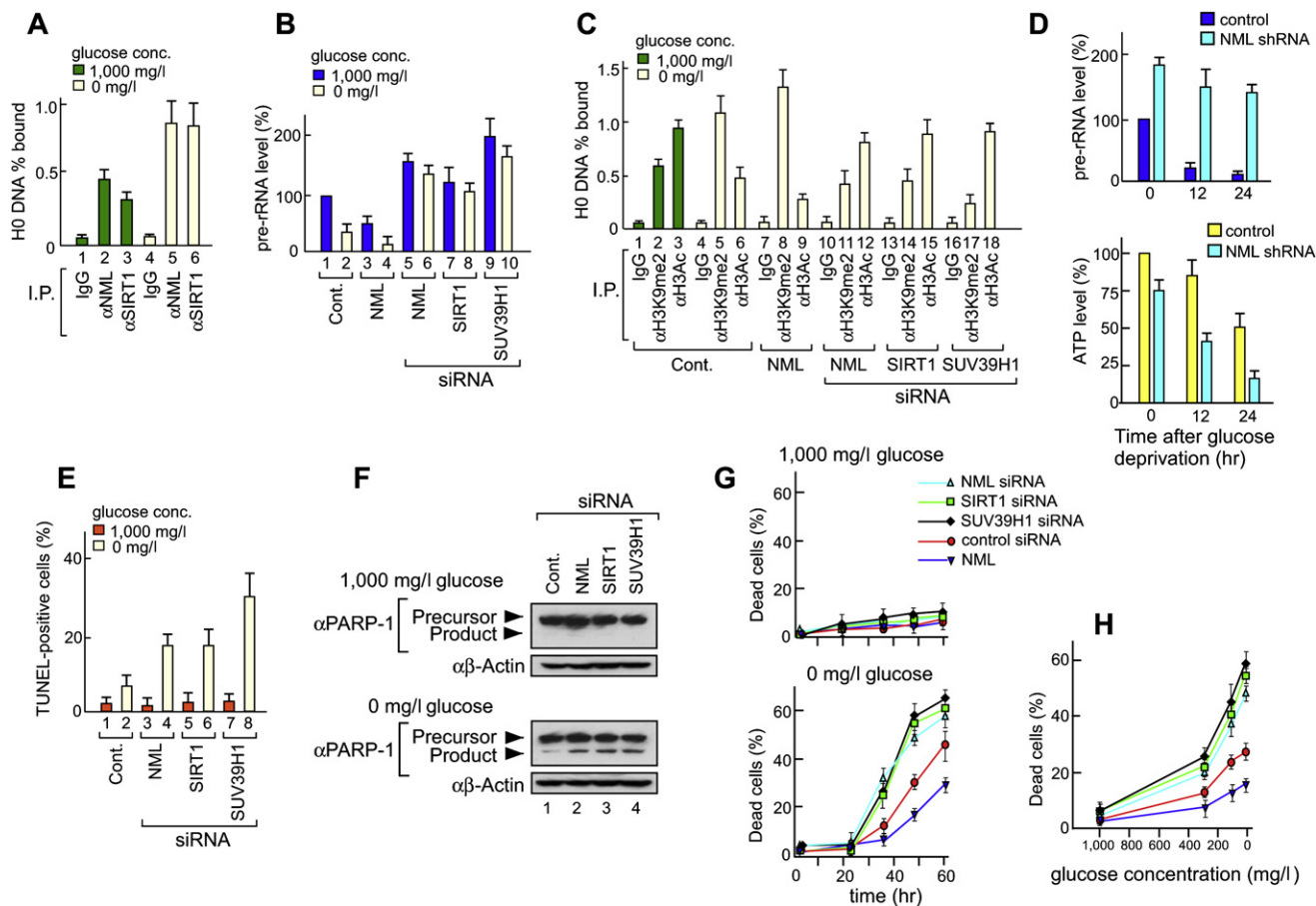
Figure 5. NML/SIRT1/SUV39H1 Complex Acts as an Energy-Dependent Repressor of rRNA Transcription and Protects Cells from Apoptosis Induced by Low Glucose

(A) Treatment of cells with low glucose increases binding of endogenous NML and SIRT1 to rDNA. HEK293 cells were treated with 1000 mg/l or 0 mg/l glucose (glucose deprivation) medium and association of NML and SIRT1 to rDNA was analyzed by ChIP assay. Values are means ± SD for triplicates.

(B) The NML complex is required for rRNA repression in response to low glucose. Pre-rRNA levels were analyzed by RT-qPCR in HEK293 cells transfected with indicated plasmids or siRNAs after 36 hr of treatment with 1000 mg/l or 0 mg/l of glucose. Values are means ± SD for triplicates.

(C) Histone modifications at the rDNA locus change in response to glucose concentration. HEK293 cells were transfected with NML plasmid or indicated siRNAs. The transfected cells were cultured for 36 hr in medium containing 1000 mg/l or 0 mg/l of glucose. Modifications of histones at the rDNA locus were analyzed by ChIP. Values are means ± SD for triplicates.

(D) Timecourse studies of pre-rRNA levels and total cellular ATP levels in control or NML shRNA cells after glucose deprivation. Control or NML shRNA cells were cultured without glucose. At the indicated time points, pre-rRNA and ATP levels were analyzed as described in the Experimental Procedures. Values are means ± SD for triplicates.

(E and F) NML/SIRT1/SUV39H1 complex protects cells from apoptosis induced by glucose deprivation. HeLa cells were transfected with the indicated siRNAs. After 48 hr, we introduced medium either with (1000 mg/l) or without glucose. (E) These cells were cultured for an additional 48 hr and subjected to TUNEL assay. Values are means ± SD for triplicates. (F) PARP-1 cleavage was analyzed by immunoblotting with anti-PARP-1 antibody.

(G) Percentage of dead cells after glucose deprivation. Forty-eight hours after transfection with the indicated siRNAs, HEK293 cells were cultured in medium containing 1000 mg/l (upper panel) or 0 mg/l of glucose (lower panel). At the indicated times, the cell viability was measured by Trypan blue exclusion assay. Values are means ± SD for triplicates.

(H) siRNA-transfected HEK293 cells were cultured in medium with 0, 100, 300, or 1000 mg/l glucose for 48 hr. The Trypan blue exclusion assay was performed to measure the viability of the cells. Values are means ± SD for triplicates.

for the specific binding to H3K9me2 peptide (Figure S2). The C-terminal domain of NML contains consensus sequence motifs (I, post-I, II, and III) found in SAM-dependent methyltransferases (SAM-MT) (Schluckebier et al., 1995) (Figure 6A). Thus, we have solved the crystal structure of the methyltransferase-like domain of NML(242–456 amino acids [aa]) complexed with S-adenosyl-homocysteine (SAH) at 2.0 Å resolution using multiwavelength

anomalous diffraction of seleno-methionyl protein crystals (Figure 6B and Table S1). NML(242–456 aa) can be divided into two parts: a large domain and a small domain. The large domain reveals an α/β structure and adopts a well-characterized SAM-MT fold with a seven-stranded β sheet (β1–β7) with two helices (α1, α2) on one side and two helices (α3, α4) on the opposite side. The small domain, comprising three helices (αA–αC), is
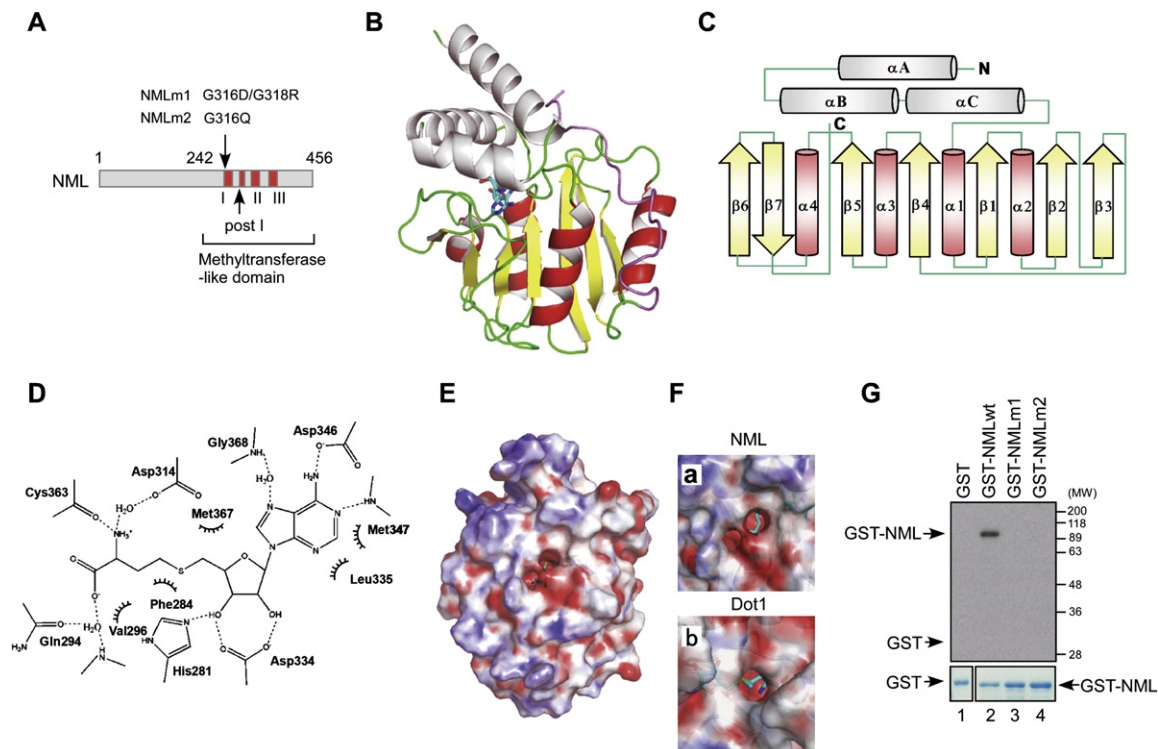
Figure 6. Structure of the Methyltransferase-like Domain of NML

(A) Schematic representation of NML and its point mutants in the methyltransferase-like domain. Conserved motifs in SAM-MTase are shown in red.

(B) Ribbon representation of methyltransferase-like domain of NML. The small domain in the N terminus is shown in gray. The bound SAH molecule is shown as a ball-and-stick model.

(C) Topological diagram of NML(242–456). Secondary structure elements are colored using the same scheme as in (B).

(D) A schematic diagram showing SAH-protein interactions. Dashed lines correspond to hydrogen bonds.

(E) Accessible surface area of NML(242–456). Solvent-accessible surface colored according to electrostatic potential in the range $-10\,k_B T$ (red) to $+10\,k_B T$ (blue), where k_B is Boltzmann's constant and T is the absolute temperature.

(F) The SAH binding pocket of (a) NML and (b) Dot1.

(G) Mutations in the NML methyltransferase-like domain lead to loss of SAM binding. Recombinant wild-type NML or its mutants were mixed with ^{3}H-labeled SAM and crosslinked by UV irradiation. ^{3}H-labeled SAM bound to protein was analyzed by SDS-PAGE followed by autoradiography (upper panel). Lower panel shows Coomassie blue staining of the same gel.

stabilized by hydrophobic interactions and packs against the SAM-MT fold via hydrophobic interactions (Figure 6C). It should be noted that the C-terminal region after β7 turns back toward the molecule and is inserted into the pocket formed by α3 and α4.

The SAH molecule is well-ordered in the crystal structure at the carboxyl ends of the parallel strands, and its three moieties are recognizable (Figure 6D). The amino group of the methionine moiety interacts with the oxygen atom of Cys363 and the carboxylate of Asp314 via a water molecule belonging to motif I. Both hydroxyls of the ribose moiety are recognized by Asp334 and His281, which belong to the post-I and small domains, respectively. Finally, the nitrogen atoms of the adenine moiety (N1, N6, and N7) interact, respectively, with the main-chain nitrogen atom of Met347, the carboxylate of Asp346, and (via a water molecule) the main-chain nitrogen atom of Gly368. The small domain forms a lid covering the SAH-binding pocket (Figure 6E). As a consequence, the pocket is almost buried, and the sulfur atom in SAH is thus only accessible via a narrow entrance (Figure 6F).

Next, to investigate whether SAM binding to NML is essential for its function, we generated two types of mutated NML, NMLm1 and NMLm2, in which the Gly residues in motif I are mutated (G316D and G318R for NMLm1 and G316Q for NMLm2) (Figure 6A). Neither mutant possesses the ability to bind SAM (Figure 6G). The aa substitutions introduced into these mutants do not affect NML binding to either SIRT1, SUV39H1, or chromatin (Figures 7A–7C). However, neither mutant was able to suppress pre-rRNA levels when expressed in HEK293 (Figure 7D) or HeLa cells (data not shown). Consistent with this, expression of the mutants did not alter the modifications of histones in rRNA genes (Figure 7E). Furthermore, NML expression protected cells from energy starvation-induced apoptosis, whereas neither mutant could do so (Figures 7F and S8), suggesting that SAM binding to NML is essential for its function. Considering that NML has a methyltransferase-like domain, it is possible that there may be target molecules of NML that are important for silencing of rDNA locus.

DISCUSSION

Our observations suggest that CR-induced changes in the NAD$^+$/NADH ratio regulate eNoSC, enabling the complex to
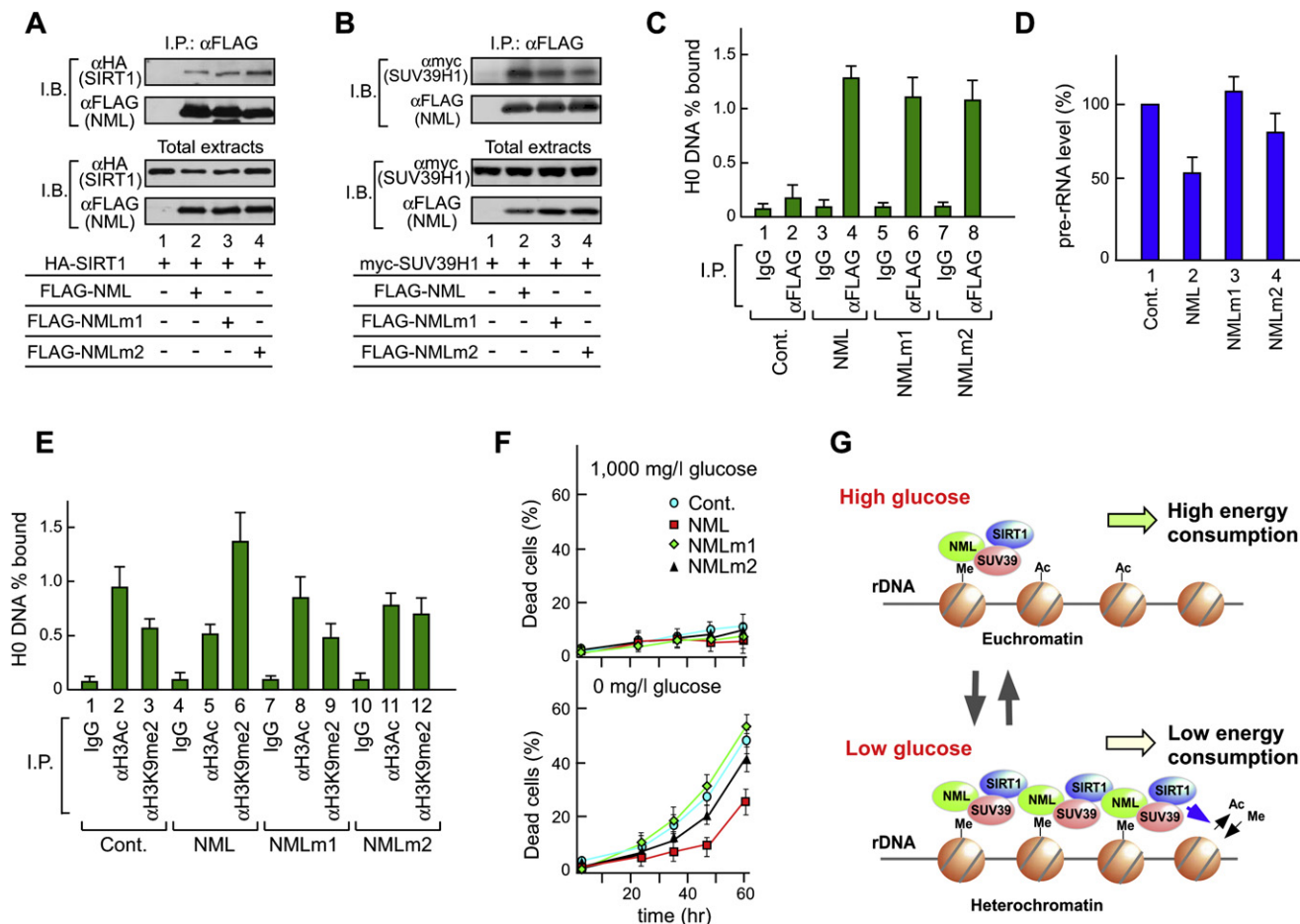
Figure 7. The Methyltransferase-like Domain of NML Plays an Essential Role in the Repression of rRNA Transcription

(A and B) The NML mutants interact with both SIRT1 and SUV39H1. HEK293 cells were transfected with FLAG-NML, FLAG-NMLm1, or FLAG-NMLm2 in combination with HA-SIRT1 (A) or myc-SUV39H1 (B) as indicated. After 24 hr, lysates were immunoprecipitated with anti-FLAG antibody and immunoblotted with the indicated antibodies.

(C) NML mutants can associate with the rDNA locus. HEK293 cells were transfected with FLAG-NML or FLAG-NMLm plasmid. Association of NML or NMLm on the rDNA locus was analyzed by ChIP using anti-FLAG antibody. Values are means ± SD for triplicates.

(D) NML mutants are not able to reduce pre-rRNA levels. HEK293 cells were transfected with plasmid encoding NML or its mutants. Pre-rRNA level was analyzed by RT-qPCR and normalized to β-actin mRNA. Values are means ± SD for triplicates.

(E) NML mutants exhibit little effect on the histone modification on the rDNA locus. HEK293 cells were transfected with NML or NMLm plasmid. Modifications of histones at the rDNA locus were analyzed by ChIP. Values are means ± SD for triplicates.

(F) Percentage of dead cells after glucose deprivation. Forty-eight hours after transfection with the indicated expression vectors, HEK293 cells were cultured in medium containing 1000 mg/l (upper panel) or 0 mg/l of glucose (lower panel). At the indicated times, the cells viability was measured by Trypan blue exclusion assay. Values are means ± SD for triplicates.

(G) Proposed model for energy-dependent eNoSC function in the nucleolus.

couple changing energy status with levels of rRNA synthesis and ribosome production. Under standard glucose conditions, the components of eNoSC interact with the rDNA region, and knockdown of these components increases pre-rRNA levels (Figures 5A and 5B). These differences were statistically significant; statistical analysis in Figure 5B by t test revealed that the p value of control (lane 1) versus siRNA transfected cells (lanes 5, 7, and 9) was < 0.05. This result implies that the complex also has a constitutive role in rDNA silencing.

In mammals, the effect of sirtuins at the rDNA locus is complex. TAF_I68, a basal component of the Pol I transcription apparatus, is a relevant target of SIRT1 (Muth et al., 2001). We also show that SIRT1 suppresses the pre-rRNA levels in the nucleolus. On the other hand, SIRT7 is a nucleolar protein that acts as a positive regulator of Pol I transcription (Ford et al., 2006). Our results that NIA, an inhibitor of SIRT family members, abrogates the function of eNoSC raised a possibility that NML could also associate with SIRT7. However, coimmunoprecipitation assay revealed that SIRT7 was not able to bind to NML (Figure S9).

The steady-state distribution of SIRT1 is essentially nucleoplasmic, showing only a very faint nucleolar localization (Michishita et al., 2005). In immunostaining using anti-SIRT1 antibody,

we observed that a small fraction of SIRT1 is localized in the nucleolus (Figure S10). These observations imply that nucleoplasmic/nucleolar shuttling is required in order for SIRT1 to act in the nucleolus. Recent evidences indicate that the nucleolus is associated with different types of protein dynamics; some nucleolar proteins such as UBF are immobile (Roussel et al., 1993), whereas other proteins such as Nucleophosmin/B23 have a steady-state nucleolar distribution but continuously shuttle between nucleolus and nucleoplasm (Colombo et al., 2002). A quantitative analysis of the proteome of nucleoli revealed that some proteins are stably copurified with nucleoli, while many proteins only accumulate transiently in nucleoli (Andersen et al., 2005). This observation also indicates that many nucleolar proteins cycle between the nucleolus and nucleoplasm. SIRT1 could be one of these proteins. Our observations demonstrate that SIRT1 functions in the nucleolus; however, we acknowledge that data obtained from overexpression experiments could include artifacts caused by forced recruitment of nucleoplasmic SIRT1 to the nucleolus.

SIRT1 has been shown to protect against apoptosis by deacetylating nonhistone proteins such as p53 (Luo et al., 2001). Therefore, it is possible that eNoSC could also inhibit cell death via deacetylating nonhistone proteins. In our hands, SIRT1-dependent p53 deacetylation was not affected by NML expression (Figure S11). In addition, NML is predominantly localized in the nucleolus. These results suggest that a major mechanism by which eNoSC protects cells from energy deprivation-induced apoptosis is rDNA silencing. However, there remains the possibility that eNoSC protects cells from apoptosis via other pathways as well.

Recent evidence indicates that SIRT1 interacts with SUV39H1 and suggests that they are functionally interrelated (Vaquero et al., 2007). In coimmunoprecipitation experiments, we also observed an interaction between SIRT1 and SUV39H1. The expression levels of NML do not affect the association between SIRT1 and SUV39H1 (Figure S12A), although the recruitment of these proteins to the rDNA region does require NML (Figures 3F and S12B). GST pull-down experiments showed that SUV39H1, but not SIRT1, binds NML in vitro (Figure S13A), suggesting that SIRT1 binds to NML through SUV39H1. We also found that glucose deprivation increases the affinity between SIRT1 and SUV39H1 (Figure S13B) and consequently strengthens the interaction between NML and SIRT1 (Figure S13C). Therefore, glucose deprivation reduces pre-rRNA levels partly due to the enhancement of affinity between SIRT1 and SUV39H1. Considering these results together with the report that SIRT1 deacetylates SUV39H1 (Vaquero et al., 2007), it is possible that the acetylation status of SUV39H1 affects the interaction between SIRT1 and SUV39H1.

Recent accumulating evidence clearly indicates that epigenetic mechanisms control rRNA gene transcription (McStay, 2006; Preuss and Pikaard, 2007). NoRC mediates rDNA silencing by recruiting DNA methyltransferase and histone deacetylase activity to rRNA promoters, thus establishing the structural characteristics of heterochromatin (Santoro and Grummt, 2005; Santoro et al., 2002). NoRC is recruited to T_0, which is a terminator element located immediately upstream of the rRNA gene promoter, via TTF-1 (Strohner et al., 2001). Thus, there remains an unsolved issue: how does silencing, established at the promoter, spread across the repeat? eNoSC might provide the mechanism: since eNoSC can change acetylation of Lys9 residue of histone H3 to dimethylation, which NML can in turn recognize and bind, the complex is potentially able to spread across the repeat (Figure 7G). However, there is a possibility that eNoSC requires silencing initiators, which would dictate which regions are silenced. Considering our results, together with previous reports, it is possible that eNoSC and NoRC may coordinately regulate the establishment of rDNA silencing, according to cellular energy status. Furthermore, NML is a human homolog of yeast Rrp8p, which is involved in cleavage of rRNA in yeast (Bousquet-Antonelli et al., 2000). Therefore, it is possible that eNoSC may also connect rRNA processing with intracellular energy status.

The sequence and structural features of NML strongly suggest that NML would be a methyltransferase, but the substrate of NML has not yet been identified. The surface representation of NML shows that SAH is accessible only via an opening to a narrow pocket. NML's narrow entrance is structurally quite similar to that of Dot1 (Min et al., 2003), an evolutionarily conserved SAM-dependent histone methyltransferase that methylates Lys79 of histone H3 in the core domain (Ng et al., 2002). Dot1 requires additional basic residues outside of the catalytic domain for its H3 methylation activity (Sawada et al., 2004). Likewise, NML also has basic residues outside of its methyltransferase-like domain. However, we could not detect any methyltransferase activity when NML was incubated with histones (Figure S14). A recent report indicates that Dot1-mediated H3K79 methylation requires the basic patch residues ($R_{17}H_{18}R_{19}$) in the N-terminal tail of histone H4 (Fingerman et al., 2007). Thus, NML may also require the N-terminal tail or modified N-terminal tail for target methylation. Alternatively, the binding of NML to components of eNoSC might induce a conformational change and make the entrance wide enough to bind and methylate nonhistone proteins; another possibility is that the target residue(s) could be aa other than Lys. Because SAM binding to NML is necessary for eNoSC-mediated rDNA silencing, it will be of great interest to identify the target of the methylation activity.

EXPERIMENTAL PROCEDURES

Cell Culture and Treatments

NB1RGB normal human neonatal skin fibroblast cells were obtained from Riken Cell Bank (Tsukuba, Japan) and maintained in αMEM (Sigma, St. Louis, MO). HeLa human cervical carcinoma cells, HEK293 human kidney epithelial cells, and HCT116 human colorectal cancer cells were maintained in DMEM (Sigma). All media were supplemented with 10% fetal bovine serum (FBS) and penicillin-streptomycin mixed solution (Nacalai tesque, Kyoto, Japan). Cells were maintained at 37°C in an atmosphere containing 5% CO_2 and 100% humidity. We used medium containing 1000 mg/l glucose, unless otherwise indicated in the figure legend.

Treatments with trichostatin A (TSA) (40 nM) or NIA (5 mM) were performed for 6 hr. For glucose treatment, cells were washed twice with PBS(−) and cultured in medium containing 10% FBS with 0 mg/l, 100 mg/l, 300 mg/l, or 1000 mg/l glucose as described in figure legends.

Antibodies

Rabbit anti-human NML antibody was raised against a synthetic peptide corresponding to 136–197 aa of NML. The list of the other antibodies is shown in the Supplemental Data.

Peptide Pull-Down Assay

H3 peptides used in this assay were purchased from Upstate. Nuclear extracts were prepared from HeLa S3 cells using Dignam protocol (Dignam et al., 1983), precleared with avidin beads, and incubated with H3 peptides conjugated with avidin beads (Promega) for 3 hr at 4°C. About 5 μg of peptide and 10^8 cells were used for one assay. The beads were then washed eight times with buffer containing 20 mM HEPES (pH 7.9), 300 mM KCl, 0.2% Triton X-100, 1 mM PMSF, and protease inhibitor cocktail (Nacalai tesque). The final wash was performed with buffer containing 4 mM HEPES (pH 7.9), 10 mM NaCl, 1 mM PMSF, and protease inhibitor cocktail. Bound proteins were eluted from the resin twice with 100 mM glycine (pH 2.8). The eluates were combined, neutralized with 1/10 volume of 1 M Tris (pH 8.0), and analyzed by SDS-PAGE.

Nucleosome-Binding Assay

Mononucleosomal fraction purified from HeLa NML stable cells was subjected to immunoprecipitation using anti-FLAG M2-agarose beads (Sigma). Eluates were analyzed by immunoblotting using anti-H3K4me2 and anti-H3K9me2 antibodies. Details are provided in the Supplemental Data.

Chromatin Immunoprecipitation and qPCR Detection

ChIP assays were performed using ChIP assay kit (Upstate) according to manufacturer's protocol. Primer sequences and experimental details are provided in the Supplemental Data.

RNA Purification and RT-qPCR

Total RNA was isolated with Sepasol RNA I Super reagent (Nacalai tesque) and reverse transcribed with SuperScript III reverse transcriptase (Invitrogen). Real-time quantitative PCR analysis was performed using the Thermal Cycler Dice TP800 (Takara) and Platinum SYBR Green qPCR SuperMix-UDG (Invitrogen). Primers and experimental details are provided in the Supplemental Data.

Metabolic Labeling

HeLa cells were labeled for 2 hr with 100 μCi of ^{35}S-methionine in methionine-free DMEM medium (GIBCO) supplemented with 10% dialyzed serum. The incorporation of ^{35}S-methionine into protein was determined using a Beckmann Coulter liquid scintillation counter and normalized to the protein content. Details are provided in the Supplemental Data.

ATP Measurement

Intracellular ATP was measured by using ATP Bioluminescence Assay Kit CLS II (Roche) and a luminometer (Berthold). ATP levels were normalized to protein content using the BCA Protein assay kit (PIERCE). Details are provided in the Supplemental Data.

Assays for Apoptosis Detection

Apoptosis was detected by TUNEL and PARP-1 cleavage analysis. Details are provided in the Supplemental Data.

Crystallization and Data Collection

NML(242–456) and SeMet-labeled NML(242–456) were successfully crystallized by the hanging-drop vapor-diffusion method, using 30% PEG8000 as a precipitant in 0.1 M MES buffer (pH 6.0) containing 200 mM ammonium sulfate. X-ray diffraction data were collected at 100K on beamline BL41 at Spring8, Japan and on beamline BL5 at The Photon Factory, Japan. Details are provided in the Supplemental Data.

Structure Determination and Refinement

The structure of NML(242–456) was solved by multiwavelength anomalous diffraction (MAD) using the SeMet-labeled NML(242–456) crystal. Details for structure determination and refinement are provided in the Supplemental Data. The final refinement statistics are summarized in Table S1.

ACCESSION NUMBERS

The KIAA0409 protein sequence was deposited in GenBank with accession number O43159. Coordinates and structure factors for NML(242–456) have been deposited in the Protein Data Bank with accession number 2ZFU.

SUPPLEMENTAL DATA

Supplemental Data include Supplemental Experimental Procedures, one table, and fourteen figures and can be found with this article online at http://www.cell.com/cgi/content/full/133/4/627/DC1/.

REFERENCES

Andersen, J.S., Lam, Y.W., Leung, A.K., Ong, S.E., Lyon, C.E., Lamond, A.I., and Mann, M. (2005). Nucleolar proteome dynamics. Nature 433, 77–83.

Bhaskar, P.T., and Hay, N. (2007). The two TORCs and Akt. Dev. Cell 12, 487–502.

Bousquet-Antonelli, C., Vanrobays, E., Gelugne, J.P., Caizergues-Ferrer, M., and Henry, Y. (2000). Rrp8p is a yeast nucleolar protein functionally linked to Gar1p and involved in pre-rRNA cleavage at site A2. RNA 6, 826–843.

Buck, S.W., Sandmeier, J.J., and Smith, J.S. (2002). RNA polymerase I propagates unidirectional spreading of rDNA silent chromatin. Cell 111, 1003–1014.

Claypool, J.A., French, S.L., Johzuka, K., Eliason, K., Vu, L., Dodd, J.A., Beyer, A.L., and Nomura, M. (2004). Tor pathway regulates Rrn3p-dependent recruitment of yeast RNA polymerase I to the promoter but does not participate in alteration of the number of active genes. Mol. Biol. Cell 15, 946–956.

Cohen, H.Y., Miller, C., Bitterman, K.J., Wall, N.R., Hekking, B., Kessler, B., Howitz, K.T., Gorospe, M., de Cabo, R., and Sinclair, D.A. (2004). Calorie restriction promotes mammalian cell survival by inducing the SIRT1 deacetylase. Science 305, 390–392.

Colombo, E., Marine, J.C., Danovi, D., Falini, B., and Pelicci, P.G. (2002). Nucleophosmin regulates the stability and transcriptional activity of p53. Nat. Cell Biol. 4, 529–533.

Dignam, J.D., Lebovitz, R.M., and Roeder, R.G. (1983). Accurate transcription initiation by RNA polymerase II in a soluble extract from isolated mammalian nuclei. Nucleic Acids Res. 11, 1475–1489.

Fingerman, I.M., Li, H.C., and Briggs, S.D. (2007). A charge-based interaction between histone H4 and Dot1 is required for H3K79 methylation and telomere silencing: identification of a new trans-histone pathway. Genes Dev. 21, 2018–2029.

Ford, E., Voit, R., Liszt, G., Magin, C., Grummt, I., and Guarente, L. (2006). Mammalian Sir2 homolog SIRT7 is an activator of RNA polymerase I transcription. Genes Dev. 20, 1075–1080.

Grummt, I. (2003). Life on a planet of its own: regulation of RNA polymerase I transcription in the nucleolus. Genes Dev. 17, 1691–1702.

Guarente, L. (2000). Sir2 links chromatin silencing, metabolism, and aging. Genes Dev. 14, 1021–1026.

Guarente, L., and Picard, F. (2005). Calorie restriction–the SIR2 connection. Cell 120, 473–482.

Hardie, D.G. (2004). The AMP-activated protein kinase pathway–new players upstream and downstream. J. Cell Sci. 117, 5479–5487.

Inoki, K., Zhu, T., and Guan, K.L. (2003). TSC2 mediates cellular energy response to control cell growth and survival. Cell *115*, 577–590.

Lachner, M., and Jenuwein, T. (2002). The many faces of histone lysine methylation. Curr. Opin. Cell Biol. *14*, 286–298.

Luo, J., Nikolaev, A.Y., Imai, S., Chen, D., Su, F., Shiloh, A., Guarente, L., and Gu, W. (2001). Negative control of p53 by Sir2alpha promotes cell survival under stress. Cell *107*, 137–148.

McStay, B. (2006). Nucleolar dominance: a model for rRNA gene silencing. Genes Dev. *20*, 1207–1214.

Mekhail, K., Rivero-Lopez, L., Khacho, M., and Lee, S. (2006). Restriction of rRNA synthesis by VHL maintains energy equilibrium under hypoxia. Cell Cycle *5*, 2401–2413.

Michishita, E., Park, J.Y., Burneskis, J.M., Barrett, J.C., and Horikawa, I. (2005). Evolutionarily conserved and nonconserved cellular localizations and functions of human SIRT proteins. Mol. Biol. Cell *16*, 4623–4635.

Min, J., Feng, Q., Li, Z., Zhang, Y., and Xu, R.M. (2003). Structure of the catalytic domain of human DOT1L, a non-SET domain nucleosomal histone methyltransferase. Cell *112*, 711–723.

Moss, T., Langlois, F., Gagnon-Kugler, T., and Stefanovsky, V. (2007). A housekeeper with power of attorney: the rRNA genes in ribosome biogenesis. Cell. Mol. Life Sci. *64*, 29–49.

Muramatsu, M., and Busch, H. (1964). Studies on nucleolar Rna of the walker 256 carcinosarcoma and the liver of the rat. Cancer Res. *24*, 1028–1034.

Muth, V., Nadaud, S., Grummt, I., and Voit, R. (2001). Acetylation of TAF(I)68, a subunit of TIF-IB/SL1, activates RNA polymerase I transcription. EMBO J. *20*, 1353–1362.

Nemoto, S., Fergusson, M.M., and Finkel, T. (2004). Nutrient availability regulates SIRT1 through a forkhead-dependent pathway. Science *306*, 2105–2108.

Ng, H.H., Feng, Q., Wang, H., Erdjument-Bromage, H., Tempst, P., Zhang, Y., and Struhl, K. (2002). Lysine methylation within the globular domain of histone H3 by Dot1 is important for telomeric silencing and Sir protein association. Genes Dev. *16*, 1518–1527.

Oakes, M.L., Siddiqi, I., French, S.L., Vu, L., Sato, M., Aris, J.P., Beyer, A.L., and Nomura, M. (2006). Role of histone deacetylase Rpd3 in regulating rRNA gene transcription and nucleolar structure in yeast. Mol. Cell. Biol. *26*, 3889–3901.

Preuss, S., and Pikaard, C.S. (2007). rRNA gene silencing and nucleolar dominance: insights into a chromosome-scale epigenetic on/off switch. Biochim. Biophys. Acta *1769*, 383–392.

Roussel, P., Andre, C., Masson, C., Geraud, G., and Hernandez-Verdun, D. (1993). Localization of the RNA polymerase I transcription factor hUBF during the cell cycle. J. Cell Sci. *104*, 327–337.

Sandmeier, J.J., French, S., Osheim, Y., Cheung, W.L., Gallo, C.M., Beyer, A.L., and Smith, J.S. (2002). RPD3 is required for the inactivation of yeast ribosomal DNA genes in stationary phase. EMBO J. *21*, 4959–4968.

Santoro, R., and Grummt, I. (2005). Epigenetic mechanism of rRNA gene silencing: temporal order of NoRC-mediated histone modification, chromatin remodeling, and DNA methylation. Mol. Cell. Biol. *25*, 2539–2546.

Santoro, R., Li, J., and Grummt, I. (2002). The nucleolar remodeling complex NoRC mediates heterochromatin formation and silencing of ribosomal gene transcription. Nat. Genet. *32*, 393–396.

Sawada, K., Yang, Z., Horton, J.R., Collins, R.E., Zhang, X., and Cheng, X. (2004). Structure of the conserved core of the yeast Dot1p, a nucleosomal histone H3 lysine 79 methyltransferase. J. Biol. Chem. *279*, 43296–43306.

Schluckebier, G., O'Gara, M., Saenger, W., and Cheng, X. (1995). Universal catalytic domain structure of AdoMet-dependent methyltransferases. J. Mol. Biol. *247*, 16–20.

Shankaranarayana, G.D., Motamedi, M.R., Moazed, D., and Grewal, S.I. (2003). Sir2 regulates histone H3 lysine 9 methylation and heterochromatin assembly in fission yeast. Curr. Biol. *13*, 1240–1246.

Shaw, R.J., Kosmatka, M., Bardeesy, N., Hurley, R.L., Witters, L.A., DePinho, R.A., and Cantley, L.C. (2004). The tumor suppressor LKB1 kinase directly activates AMP-activated kinase and regulates apoptosis in response to energy stress. Proc. Natl. Acad. Sci. USA *101*, 3329–3335.

Strohner, R., Nemeth, A., Jansa, P., Hofmann-Rohrer, U., Santoro, R., Langst, G., and Grummt, I. (2001). NoRC–a novel member of mammalian ISWI-containing chromatin remodeling machines. EMBO J. *20*, 4892–4900.

Tiainen, M., Ylikorkala, A., and Makela, T.P. (1999). Growth suppression by Lkb1 is mediated by a G(1) cell cycle arrest. Proc. Natl. Acad. Sci. USA *96*, 9248–9251.

Vaquero, A., Scher, M., Lee, D., Erdjument-Bromage, H., Tempst, P., and Reinberg, D. (2004). Human SirT1 interacts with histone H1 and promotes formation of facultative heterochromatin. Mol. Cell *16*, 93–105.

Vaquero, A., Scher, M., Erdjument-Bromage, H., Tempst, P., Serrano, L., and Reinberg, D. (2007). SIRT1 regulates the histone methyl-transferase SUV39H1 during heterochromatin formation. Nature *450*, 440–444.

Yang, T., Fu, M., Pestell, R., and Sauve, A.A. (2006). SIRT1 and endocrine signaling. Trends Endocrinol. Metab. *17*, 186–191.

Yuan, X., Feng, W., Imhof, A., Grummt, I., and Zhou, Y. (2007). Activation of RNA polymerase I transcription by cockayne syndrome group B protein and histone methyltransferase G9a. Mol. Cell *27*, 585–595.